5

BROWNIAN MOTION AND THERMOPHORESIS EFFECTS ON VISCOELASTIC FLUID FLOW

Content of this chapter is communicated.

BROWNIAN MOTION AND THERMOPHORESIS EFFECTS ON VISCOELASTIC FLUID FLOW

There are several physical and practical situations that are directly related to fluid flow and heat transfer produced by stretching/shrinking sheet. The uses of such types of mechanisms are involved in industrial and engineering simulations of fluid transport due to stretching/shrinking. This investigation embraces the study two-dimensional viscoelastic fluid flow over a stretchable surface. The analysis is performed considering Brownian motion, chemical reaction, and thermophoresis into account.

5.1 Introduction of the problem:

Viscoelastic fluid behavior is a type of non-Newtonian fluid formed by a viscous component and an elastic one. Examples of viscoelastic fluids are paints, some biological fluids, and DNA suspensions, etc. The importance of viscoelastic A number of features make the viscoelastic fluids very interesting and of industrial importance. A proper understanding of viscoelasticity is key for industrial applications. Viscoelastic fluids are common in very important applications [121, 125, and 163]. Research works in the MHD have been advanced significantly during the last few years in natural sciences and engineering disciplines after the pioneer work of Hartmann [52] in liquid metal duct flows under the influence of an external magnetic field. Recently, many researchers done works on MHD flow of viscoelastic fluid [7, 110, and 161]. The radiation effects become much vital when the difference between the surface and the ambient temperatures is extensive. It has wide applications in manufacturing industries, such as the design of reliable equipment, nuclear plants, gas turbines, power plants, and various propulsion devices for aircraft and missiles. Further, the radiation effects on MHD convective flow problems are more significant in electrical power generation, solar power technology, and astrophysical ground. Recently, Mittal and Kataria [5] studied fluid flow in the presence of radiation whereas, Non-linear thermal radiation effects on MHD flow with heat and mass transfer are also important in engineering fields. The effects of non-linear thermal radiation on MHD flow with different fluid are discussed in Ref. [33, 48]. The study of chemical reaction procedures is beneficial for improving a number of chemical technologies, such as food processing, polymer production, and manufacturing of ceramics or glassware. Kataria and Patel [43] studied the effects of chemical

reaction on magnetohydrodynamic Casson fluid flow over an exponentially accelerated vertical plate. Hayat et al. [145] and Ramesh [21] considered chemical reaction effects on viscoelastic fluid flow problems. Owing to the significance of thermal radiation and chemical reactions effects on fluid flow, extensive research works [104, 108, 139, and 142] are carried out. Recently, Jena et al. [123] studied the Chemical reaction effect on viscoelastic fluid flow over a vertical stretching sheet whereas, Imtiaz et al. [75] discussed homogeneous-heterogeneous reactions in MHD radiative flow due to a curved stretching surface. There are several physical and practical situations that are directly related to fluid flow and heat transfer produced by stretching/shrinking sheet. The uses of such types of mechanisms are involved in industrial and engineering simulations of fluid transport due to stretching/shrinking. Such type of fluid flow models is widely discussed and summarized by [3, 4, and 14].

5.2 Novelty of the chapter:

To the best of the knowledge, till date there are no attempts to model, no investigation has been made which provides the analytic expression for the steady two-dimensional MHD flow of viscoelastic fluid over stretching/shrinking sheet considering the effects of Brownian motion, thermal radiation, and chemical reaction. Homotopy analysis method [122] is used for finding solutions to the governing equations.

5.3 Mathematical Formulation of the Problem:

Two-dimensional incompressible steady viscoelastic fluid over a stretching/shrinking surface is considered. The origin is taken as stagnation point. Plate is assumed to be along $x-axis$, and is subject to forces of magnitude bx applied in opposite directions keeping origin fixed which is represented in Figures 5.1. Flow is along positive y direction. Components of velocity along x and $y-axis$ are assumed to be u and v respectively. Here we assign a magnetic field perpendicular to the stretching sheet.

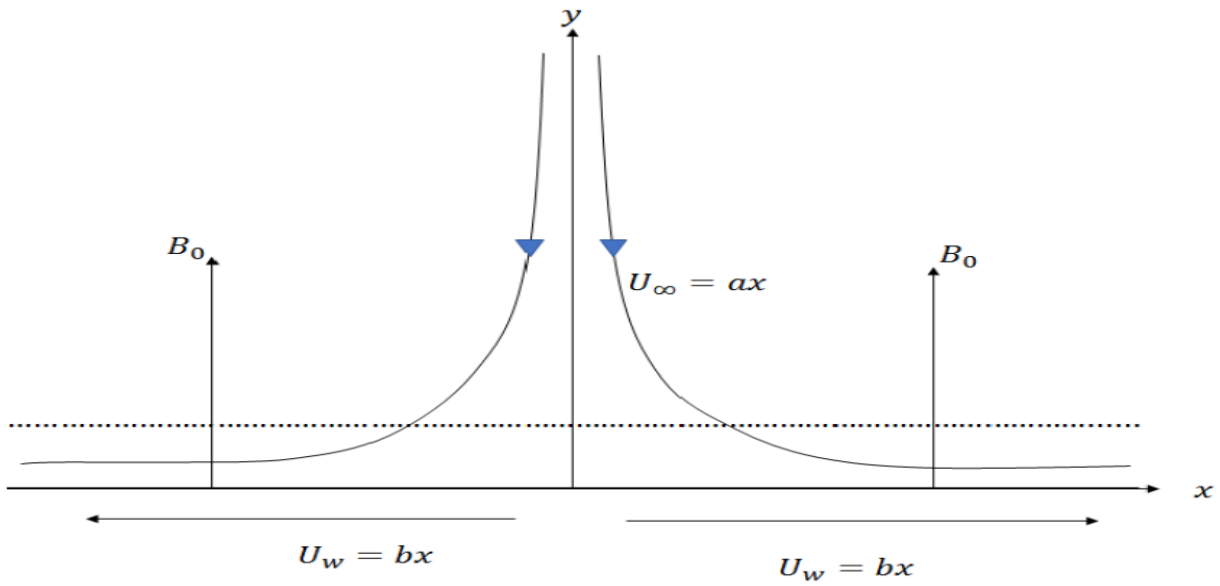

Figure 5.1: Physical sketch of the problem

The governing equations are:

$$\frac{\partial u}{\partial x} + \frac{\partial v}{\partial y} = 0, \tag{5.1}$$

$$u\frac{\partial u}{\partial x} + v\frac{\partial v}{\partial y} = U_\infty \frac{dU_\infty}{dx} + v\frac{\partial^2 u}{\partial y^2} - \frac{\sigma B_0^2}{\rho}\left(u + k_0 v\frac{\partial u}{\partial y}\right) - k_0\left(u^2\frac{\partial^2 u}{\partial x^2} + v^2\frac{\partial^2 u}{\partial y^2} + 2uv\frac{\partial^2 u}{\partial x \partial y}\right) \tag{5.2}$$

$$u\frac{\partial T}{\partial x} + v\frac{\partial T}{\partial y} = \frac{k}{\rho c_p}\left(\frac{\partial^2 T}{\partial y^2}\right) - \frac{1}{\rho c_p}\frac{\partial q_r}{\partial y} + D_B\left(\frac{\partial C}{\partial y}\frac{\partial T}{\partial y}\right) + \left(\frac{D_T}{T_\infty}\right)\left(\frac{\partial T}{\partial y}\right)^2 \tag{5.3}$$

$$u\frac{\partial C}{\partial x} + v\frac{\partial C}{\partial y} = \left(\frac{D_T}{T_\infty}\right)\left(\frac{\partial^2 T}{\partial y^2}\right) - k_2'(C - C_\infty) + D_B\left(\frac{\partial^2 C}{\partial y^2}\right) \tag{5.4}$$

Where $U_\infty = ax,\ a > 0$ is the straining velocity of the flow is the straining constant, where u and v are the velocity component in the x and y directions. T_∞ and C_∞ are denoted for the ambient values of T and C, when y tends towards infinity.

The boundary conditions for the above defined model are:

$$u = U_w = bx,\ \ v = 0,\ \ -k\frac{\partial T}{\partial y} = h(T_w - T),\ \ C = C_w \quad \text{at } y = 0,$$

$$u \to U_\infty = ax, T \to T_\infty,\ \ C \to C_\infty, as\ y \to \infty. \tag{5.5}$$

Where the temperature has linear relationship with temperature gradient, T_w and C_w are the temperature of the fluid and concentration at the wall.

Heat flux is:

$$q_r = -\frac{4\sigma^*}{3k^*}\frac{\partial T^4}{\partial y} \tag{5.6}$$

The velocity components u and v are given as:

$$u = bxf'(\eta),\ v = -\sqrt{b\upsilon}f(\eta) \tag{5.7}$$

As per usual, the stream function ψ is defined as $u = \frac{\partial \psi}{\partial y}$ and $v = -\frac{\partial \psi}{\partial x}$ so that Eq. (5.1) is satisfied.

We introduce the following dimensionless quantities:

$$\eta = \sqrt{\frac{b}{\upsilon}}y,\quad \theta(\eta) = \frac{T-T_\infty}{T_w-T_\infty},\quad C(\eta) = \frac{C-C_\infty}{C_w-C_\infty},\quad \psi = \sqrt{b\upsilon}xf(n) \tag{5.8}$$

Now substituting Eqs. (5.6) - (5.8) into Eqs. (5.2) - (5.4), we get the system of non-linear ordinary differential equations as follows:

$$f''' - K(f^2f''' - 2ff'f'') + M^2Kff'' + ff'' - M^2f' = f'^2 - s^2, \tag{5.9}$$

$$(1+R)\theta'' + \Pr\left(f\theta' + Nb\theta'C' + Nt\theta'^2\right) = 0, \tag{5.10}$$

$$C'' + LePr(fC' - Kr\,C) + \frac{Nt}{Nb}\theta'' = 0. \tag{5.11}$$

where derivatives denote differentiation with respect to η and the transformed boundary conditions of the problem are:

$$f'(0) = 1,\qquad f(0) = 0,\qquad \theta'(0) = -Bi\big(1-\theta(0)\big),\qquad C(0) = 1,$$

$$f'(\eta) = s,\quad \theta(\eta) = 0,\quad C(\eta) = 0,\ \text{as}\ \eta \to \infty. \tag{5.12}$$

where $M = \sqrt{\frac{\sigma B_0^2}{\rho b}}$, $s = \frac{a}{b}$, $K = k_0 b$, $Pr = \frac{\upsilon}{\alpha}$, $R = \frac{16\sigma^* T_\infty^3}{3k^*k}$, $Nb = \frac{\tau D_B(C_w-C_\infty)}{\upsilon}$,

$Nt = \frac{\tau D_T(T_w-T_\infty)}{\upsilon T_\infty}$, $Bi = \frac{\sqrt{\upsilon a}h}{ak}$, $Kr = \frac{k_2'}{C}$, $Le = \frac{k}{\rho c_p D_B}$

The Skin friction coefficient C_f, the local Nusselt numer Nu_x and the local Sherwood number Sh_x are described as follows:

$$C_f = \frac{\tau_w}{\rho U_w^2}, Nu_x = \frac{xq_w}{\alpha(T_w-T_\infty)}, Sh_x = \frac{xq_m}{D_B(C_w-C_\infty)}, \tag{5.13}$$

where T_w, q_w and q_m denotes surface shear stress, heat flux and mass flux respectively.

$$\tau_w = \mu(1+K)\left(\frac{\partial u}{\partial y}\right)_{y=0},\qquad q_w = -\alpha\left(\frac{\partial T}{\partial y}\right)_{y=0},\ q_m = -D_B\left(\frac{\partial C}{\partial y}\right)_{y=0}. \tag{5.14}$$

Using the similarity variables, we obtain

$$C_f Re_x^{1/2} = (1+K)f''(0), Re_x^{-1/2}Nu_x = -\theta'(0),\ \ Re_x^{-1/2}Sh_x = -C'(0). \tag{5.15}$$

where $Re_x = \frac{U_w x}{\upsilon}$ is the Reynolds number.

5.4 Solution by Homotopy Analysis Method:

In HAM initial guesses $f_0(\eta)$, $\theta_0(\eta)$, $C_0(\eta)$ and linear operators L_f , L_θ , L_C are chosen in such a way that they satisfy the boundary conditions given in Eq. (5.12).

The initial guess is

$$f_0(\eta) = (1 + s\eta)(1 - e^{-\eta}) \ , \qquad \theta_0(\eta) = \frac{Bi}{Bi+1}\, e^{-\eta} \qquad , C_0(\eta) = \ e^{-\eta} \tag{5.16}$$

with auxiliary linear operators

$$L_f = \frac{\partial^3 f}{\partial \eta^3} + \frac{\partial^2 f}{\partial \eta^2}, \qquad L_\theta = \frac{\partial^2 \theta}{\partial \eta^2} + \frac{\partial \theta}{\partial \eta} \ , \qquad L_\phi = \frac{\partial^2 C}{\partial \eta^2} + \frac{\partial C}{\partial \eta} \tag{5.17}$$

$$\text{with} \quad L_f(C_1 + C_2\,\eta + C_3 e^{-\eta}) = 0, \ L_\theta(C_4 + C_5 e^{-\eta}) = 0, \quad L_C(\,C_6 + C_7 e^{-\eta}) = 0. \tag{5.18}$$

where c_1, $c_2, \ldots, c_7$ "are constants.

The zeroth order deformation problems are constructed as follows:

$$(1-p)L_f\left[\hat{f}(\eta;\, p) - f_0(\eta)\right] = p\hbar_f H_f N_f\left[\hat{f}(\eta;\, p)\right], \tag{5.19}$$

$$(1-p)L_\theta\left[\hat{\theta}(\eta;\, p) - \theta_0(\eta)\right] = p\hbar_\theta H_\theta N_\theta\left[\hat{\theta}(\eta;\, p)\right], \tag{5.20}$$

$$(1-p)L_C\left[\hat{C}(\eta;\, p) - C_0(\eta)\right] = p\hbar_C H_C N_C\left[\hat{C}(\eta;\, p)\right], \tag{5.21}$$

The nonlinear operator are defined as

$$N_f\left[\hat{f}(\eta;\, p)\right] = \ \frac{\partial^3 \hat{f}}{\partial \eta^3} - K\hat{f}^2\frac{\partial^3 \hat{f}}{\partial \eta^3} + \hat{f}\frac{\partial^2 \hat{f}}{\partial \eta^2} + M^2 K\hat{f}\frac{\partial^2 \hat{f}}{\partial \eta^2} + 2K\hat{f}\ \frac{\partial \hat{f}}{\partial \eta}\frac{\partial^2 \hat{f}}{\partial \eta^2} - \left(\frac{\partial \hat{f}}{\partial \eta}\right)^2 - M^2\frac{\partial \hat{f}}{\partial \eta} + s^2, \tag{5.22}$$

$$N_\theta\left[\hat{\theta}(\eta;\, p)\right] = \ (1+R)\frac{\partial^2 \hat{\theta}}{\partial \eta^2} + Pr\hat{f}\frac{\partial \hat{\theta}}{\partial \eta} + PrNb\frac{\partial \hat{\theta}}{\partial \eta}\frac{\partial \hat{C}}{\partial \eta} + PrNt\left(\frac{\partial \hat{\theta}}{\partial \eta}\right)^2, \tag{5.23}$$

$$N_C\left[\hat{C}(\eta;\, p)\right] = \frac{\partial^2 \hat{C}}{\partial \eta^2} + LePr\hat{f}\frac{\partial \hat{C}}{\partial \eta} - KrLePr\hat{C} + \frac{Nt}{Nb}\frac{\partial^2 \hat{\theta}}{\partial \eta^2}, \tag{5.24}$$

Subject to the boundary conditions:

$$\hat{f}(\eta) = 0, \quad \hat{f}'(\eta) = 1 \ at\ \eta = 0 \quad \hat{f}'(\eta) = s \ at\ \eta \to \infty\,, \tag{5.25}$$

$$\hat{\theta}'(\eta) = -Bi\left(1 - \hat{\theta}(0)\right) at\ \eta = 0,\ \hat{\theta}(\eta) = 0\ at\ \eta \to \infty\,, \tag{5.26}$$

$$\hat{C}(\eta) = 1\ at\ \eta = 0\,, \ \hat{C}(\eta) = 0\ at\ \eta \to \infty. \tag{5.27}$$

Where $\hat{f}(\eta;\, p), \hat{\theta}(\eta;\, p)$ and $\hat{C}(\eta;\, p)$ are unknown functions with respect to η and p. $\hbar_f$, $\hbar_\theta$ and $\hbar_C$ are the non-zero auxiliary parameters and N_f, N_θ and N_C are the nonlinear operators.

Also where $p \in (0,\ 1)$ is an embedding parameter For $p = 0$ and $p = 1$ we have

$$\hat{f}(\eta; 0) = f_0(\eta), \hat{f}(\eta; 1) = f(\eta), \tag{5.28}$$

$$\hat{\theta}(\eta; 0) = \ \theta_0(\eta), \hat{\theta}(\eta; 1) = \ \theta(\eta), \tag{5.29}$$

$$\hat{C}(\eta; 0) = \ C_0(\eta), \ \hat{C}(\eta; 1) = \ C(\eta), \tag{5.30}$$

Taylor's series expansion of these functions yields the following:

$$\hat{f}(\eta;\ p) = f_0(\eta) + \sum_{m=1}^{\infty} f_m(\eta)p^m, \tag{5.31}$$

$$\hat{\theta}(\eta;\ p) = \theta_0(\eta) + \sum_{m=1}^{\infty} \theta_m(\eta)p^m, \tag{5.32}$$

$$\hat{C}(\eta;\ p) = C_0(\eta) + \sum_{m=1}^{\infty} C_m(\eta)p^m, \tag{5.33}$$

Where

$$f_m(\eta) = \frac{1}{m!}\left[\frac{\partial^m f(\eta;\ p)}{\partial p^m}\right]_{p=0}, \tag{5.34}$$

$$\theta_m(\eta) = \frac{1}{m!}\left[\frac{\partial^m \theta(\eta;\ p)}{\partial p^m}\right]_{p=0}, \tag{5.35}$$

$$C_m(\eta) = \frac{1}{m!}\left[\frac{\partial^m C(\eta;\ p)}{\partial p^m}\right]_{p=0}. \tag{5.36}$$

It should be noted that the convergence in the above series strongly depends upon $\hbar_f, \hbar_\theta$ and $\hbar_C$ and the proper functions $H_f(\eta),\ H_\theta(\eta)$ and $H_C(\eta)$. Assuming that these nonzero auxiliary parameters are chosen so that Equations (5.35)–(5.37) converges at $p = 1$, Hence one can obtain the following.

$$f(\eta) = f_0(\eta) + \sum_{m=1}^{\infty} f_m(\eta), \tag{5.37}$$

$$\theta(\eta) = \theta_0(\eta) + \sum_{m=1}^{\infty} \theta_m(\eta), \tag{5.38}$$

$$C(\eta) = C_0(\eta) + \sum_{m=1}^{\infty} C_m(\eta), \tag{5.39}$$

The m^{th} order deformation equations can be presented in the form

$$L_f[f_m(\eta) - \chi_m f_{m-1}(\eta)] = \hbar_f H_f(\eta) R_{f,m}(\eta), \tag{5.40}$$

$$L_\theta[\theta_m(\eta) - \chi_m \theta_{m-1}(\eta)] = \hbar_\theta H_\theta(\eta) R_{\theta,m}(\eta), \tag{5.41}$$

$$L_C[C_m(\eta) - \chi_m C_{m-1}(\eta)] = \hbar_C H_C(\eta) R_{C,m}(\eta), \tag{5.42}$$

Subject to the boundary conditions

$$f_m(0) = f_m'(0) = f_m'(+\infty) = 0,$$
$$\theta_m'(0) = Bi\,\theta_m(0), \qquad \theta_m(+\infty) = 0,$$
$$C_m(0) = C_m(+\infty) = 0\,, \tag{5.43}$$

$$R_{f,m}(\eta) = f_{m-1}''' - K\sum_{j=0}^{m-1} f_{m-1-j}\sum_{i=0}^{j} f_i f_{j-i}''' + \sum_{j=0}^{m-1} f_j f_{m-1-j}'' + M^2 K\sum_{j=0}^{m-1} f_j f_{m-1-j}''$$
$$+2K\sum_{j=0}^{m-1} f_{m-1-j}\sum_{i=0}^{j} f_i' f_{j-i}'' - \sum_{j=0}^{m-1} f_j' f_{m-1-j}' - M^2 f_{m-1}' + s^2(1-\chi_m) \tag{5.44}$$

$$R_{\theta,m}(\eta) = \ (1+\mathrm{R})\theta_{m-1}'' + Pr\sum_{j=0}^{m-1} f_j\theta_{m-1-j}' + PrNb\sum_{j=0}^{m-1} \theta_j' C_{m-1-j}' + PrNt\sum_{j=0}^{m-1} \theta_j'\theta_{m-1-j}'\,, \tag{5.45}$$

$$R_{\phi,m}(\eta) = \ C_{m-1}'' + LePr\sum_{j=0}^{m-1} f_j\, C_{m-1-j}' - Kr\, LePr C_{m-1} + \frac{Nt}{Nb}\,\theta_{m-1}''. \tag{5.46}$$

$$\text{with } \chi_m = \begin{cases} 0, & m \le 1 \\ 1, & m \ge 1 \end{cases}, \tag{5.47}$$

To assure the convergence, the auxiliary functions $H_f(\eta)$, $H_\theta(\eta)$, $H_C(\eta)$ are selected as

$$H_f(\eta) = H_\theta(\eta) = H_C(\eta) = e^{-\eta}. \quad (5.48)$$

The general solutions f_m, θ_m *and* C_m comprising the special solution f_m^*, θ_m^* *and* C_m^* are given by

$$f_m(\eta) = f_m^*(\eta) + C_1 + C_2\,\eta + C_3 e^{-\eta}, \quad (5.49)$$

$$\theta_m(\eta) = \theta_m^*(\eta) + C_4 + C_5 e^{-\eta}, \quad (5.50)$$

$$C_m(\eta) = C_m^*(\eta) + C_6 + C_7 e^{-\eta}. \quad (5.51)$$

Here f_m^*, θ_m^* *and* C_m^* are given by are particular solutions of the corresponding mth- order equations and the constants $C_i (\, i = 1,2, \ldots, 7)$ are to be determined by the boundary conditions.

5.4.1 Convergence Analysis

Convergence of the HAM solutions and their rate of approximations strongly depend on the values of the auxiliary parameters $\hbar_f, \hbar_\theta$ and $\hbar_C$. For this purpose, the associated h-curve is plotted in Figure 2. In the present case, H-curve of $f_0''(0)$ is plotted taking appropriate order. The Figure 5.2 clearly suggest permissible ranges for the auxiliary parameter $\hbar_f$. Similarly values for $\hbar_\theta$ and $\hbar_C$ are chosen.

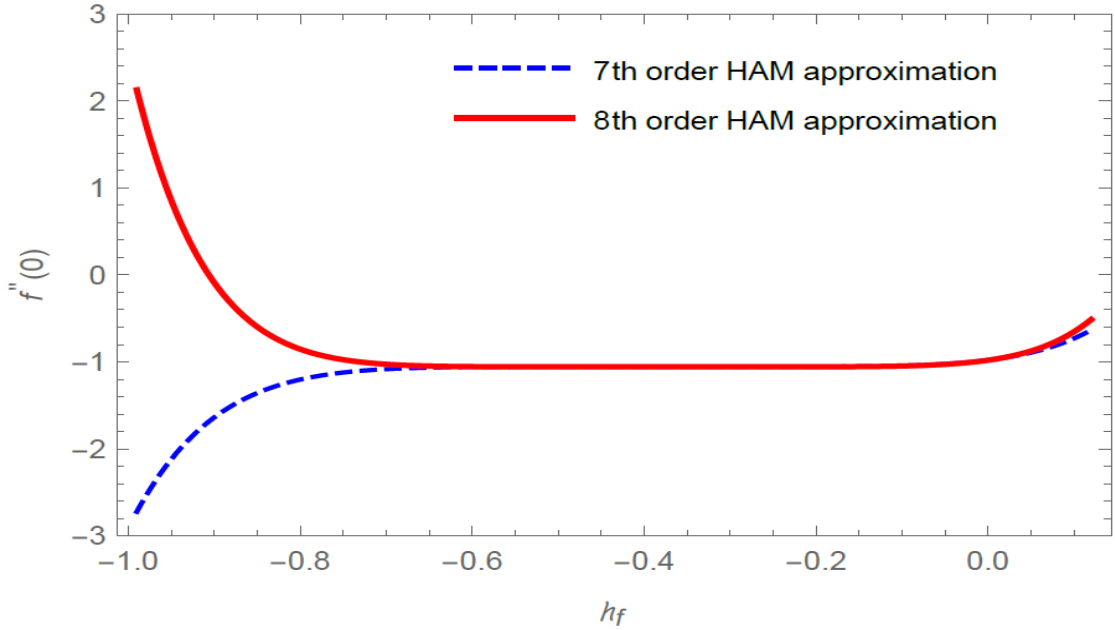

Figure 5.2: The H-Curve of $\boldsymbol{f''(0)}$ for 7th & 8th HAM approximation at $M = 1.2,\ Pr = 6.7,\ s = 0.01, Bi = 0.1, Nb = 0.2, Nt = 0.2, Le = 0.5, K = 0.05, Kr = 0.2, R = 2.0$

5.5 Results and Discussion:

Through Figures 5.3 – 5.27, the contribution of various parameter used in the system on the velocity, the temperature and the concentration distributions are deliberated in detail. Influence of the viscoelastic parameter K on the velocity profile is displayed in Figure 5.3. It can be noticed that the velocity of the fluid reduces with increases viscoelastic parameter K. Figure 5.4 describes

that the velocity drops as M increases. Physically, when we increased Magnetic parameter, means enhanced Lorentz force, which resists the flow. Figure 5.5 shows that a rise in the stagnation parameter s creates widening in the velocity profile. Variation in temperature profile θ for different values of Biot number Bi is shown in Figure 5.6. Here temperature is increasing for larger values of Biot number Bi as stronger convection yields a developed temperature profile. Figure 5.7 displays that fluid temperature increases with increase in the chemical reaction parameter Kr. Figure 5.8 depicts behavior of the Viscoelastic fluid parameter K on temperature profile. It can be noticed that temperature profile increases as the Viscoelastic fluid parameter increases. Consequence of Magnetic parameter M on the temperature profile in shown in figure 5.9. The presence of stronger Magnetic field increases the temperature profile. The effect of Nb on temperature profile is sketched in Figure 5.10. It can be observed that the temperature profile increases as Nb increases. Figure 5.11 represents that temperature rises with increase in radiation parameter R. Figure 5.12 indicates that larger values of Thermophoresis parameter Nt leads to higher temperature profile. Result of Prandtl number Pr on temperature profile is illustrated in Figure 5.13. An enhancement in the Prandtl number Pr causes decay in temperature profile. Figure 5.14 demonstrates the variation in temperature profile for different values of the stagnation parameter s. We can notice that as stagnation parameter rises, with increases temperature profile. Figure 5.15 disclosed the behavior of the Bi on the concentration profile. It is observed that increase in Biot number Bi enhances the concentration profile. Figure 5.16 shows that fluid concentration increases with increase in the chemical reaction parameter Kr. It is clear from Figure 5.17 that as the viscoelastic parameter κ increases the concentration rises. In Figure 5.18 the influence of Lewis number Le on the concentration can be seen. Here the concentration profile reduces as Lewis parameter increases. The increasing Lewis number causes to the lesser mass diffusivity so the concentration profile decreasing. In figure 5.19, concentration profile increases for large value of magnetic parameter M. It is realized from Figure 5.20 that increase in Brownian motion parameter Nb reduces the concentration, it is since Brownian motion can reduce the mass transfer.

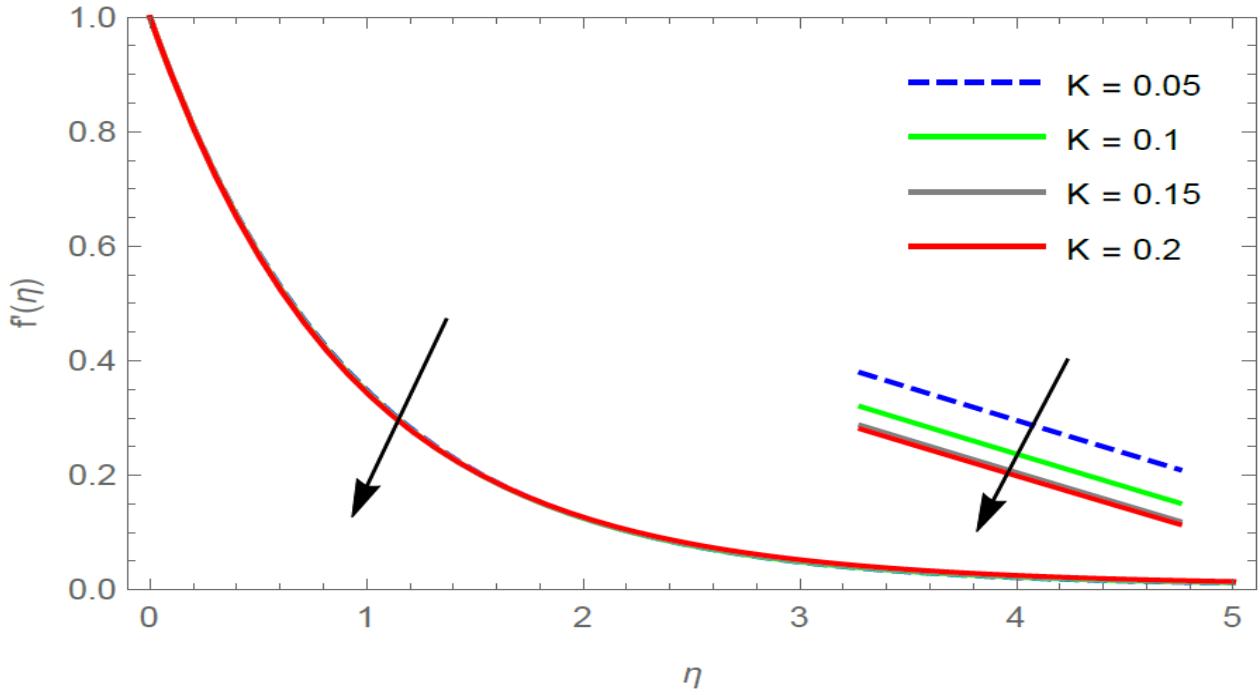

Figure 5.3: f' for η and K at $M = 1.2,\ s = 0.01,\ Pr = 6.7,\ Nb = 0.2,\ R = 2.0,\ Nt = 0.2,$ $Le = 0.5,\ Kr = 0.2,\ Bi = 1.0.$

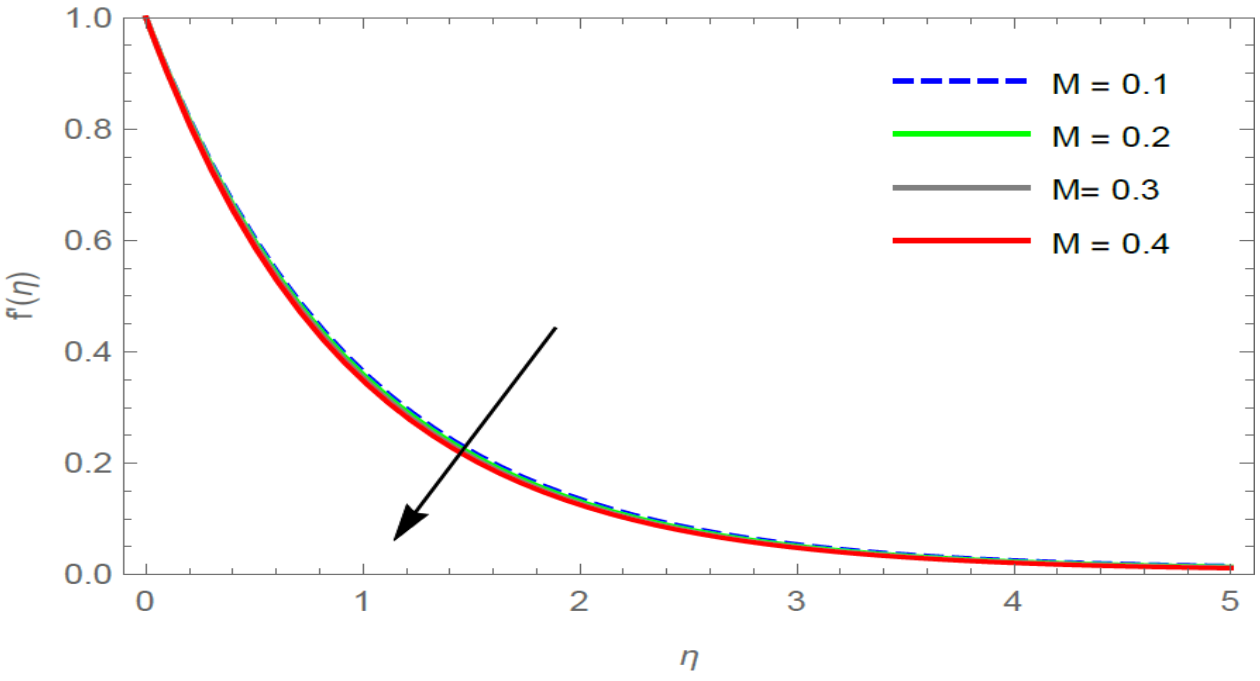

Figure 5.4: f' for $\eta\ and\ \ M$ at $K = 0.05,\ Bi = 0.1,\ s = 0.01,\ Pr = 6.7,\ Nb = 0.2,\ Nt = 0.2,$ $Le = 0.5,\ Kr = 0.2,\ R = 2.0.$

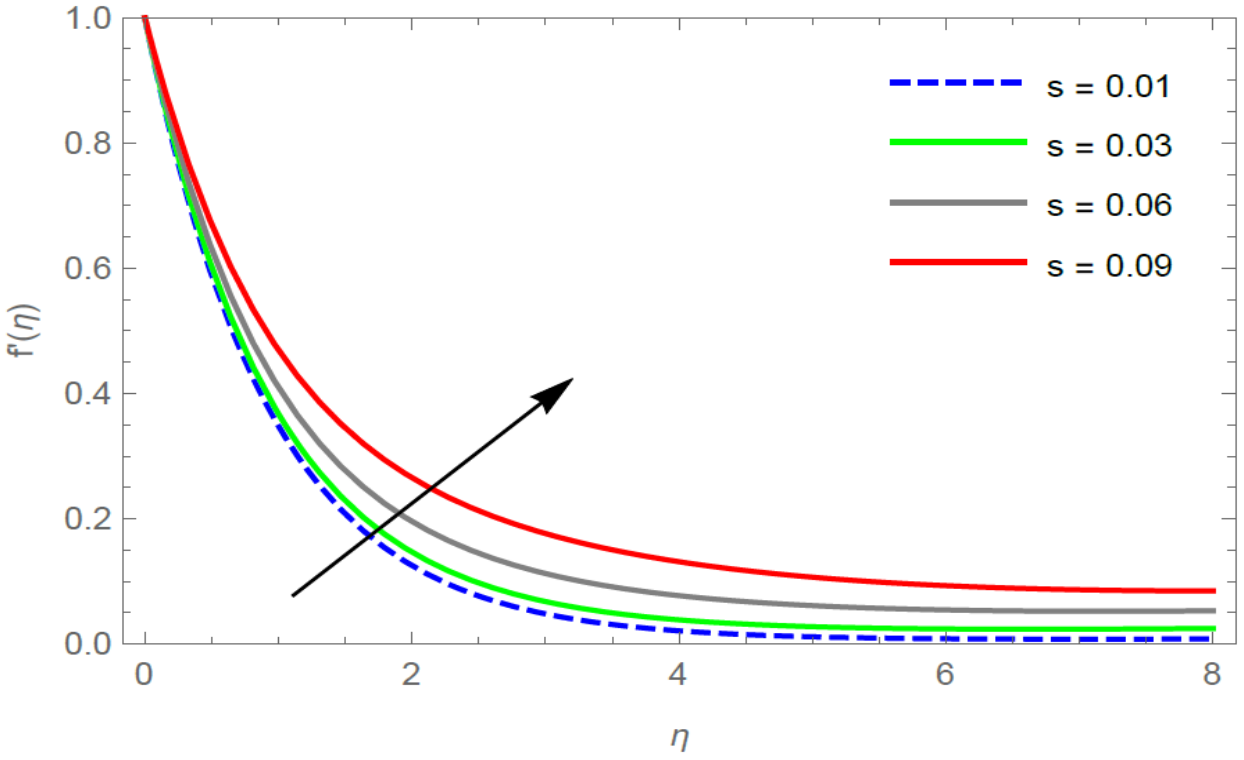

Figure 5.5: f' for η and s at $M = 0.4,\ Le = 0.5,\ Pr = 6.7,\ Nb = 0.2,\ Nt = 0.2,\ Bi = 0.1,$ $K = 0.05,\ Kr = 0.2,\ R = 2.0.$

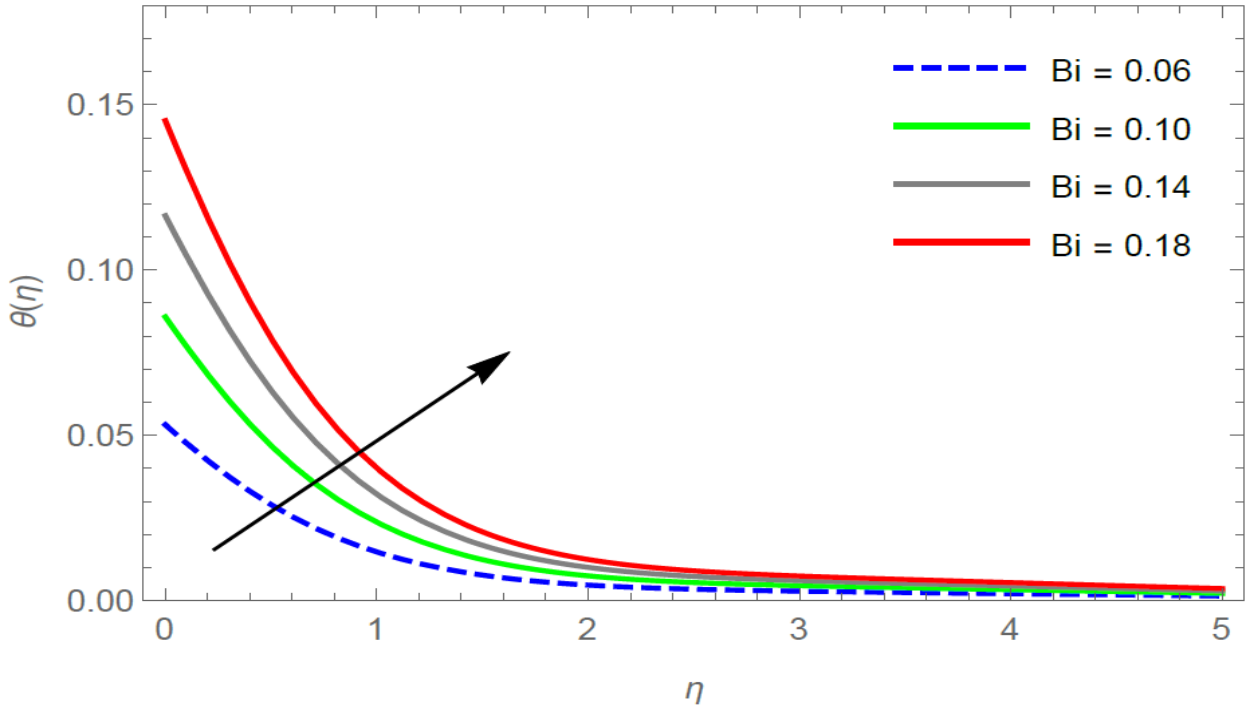

Figure 5.6: θ for $\eta\ and\ \ Bi$ at $M = 1.2,\ s = 0.01,\ Nt = 0.2,\ Nb = 0.2,\ Le = 0.5,\ K = 0.05,$ $Pr = 6.7,\ Kr = 0.2\ , R = 2.0.$

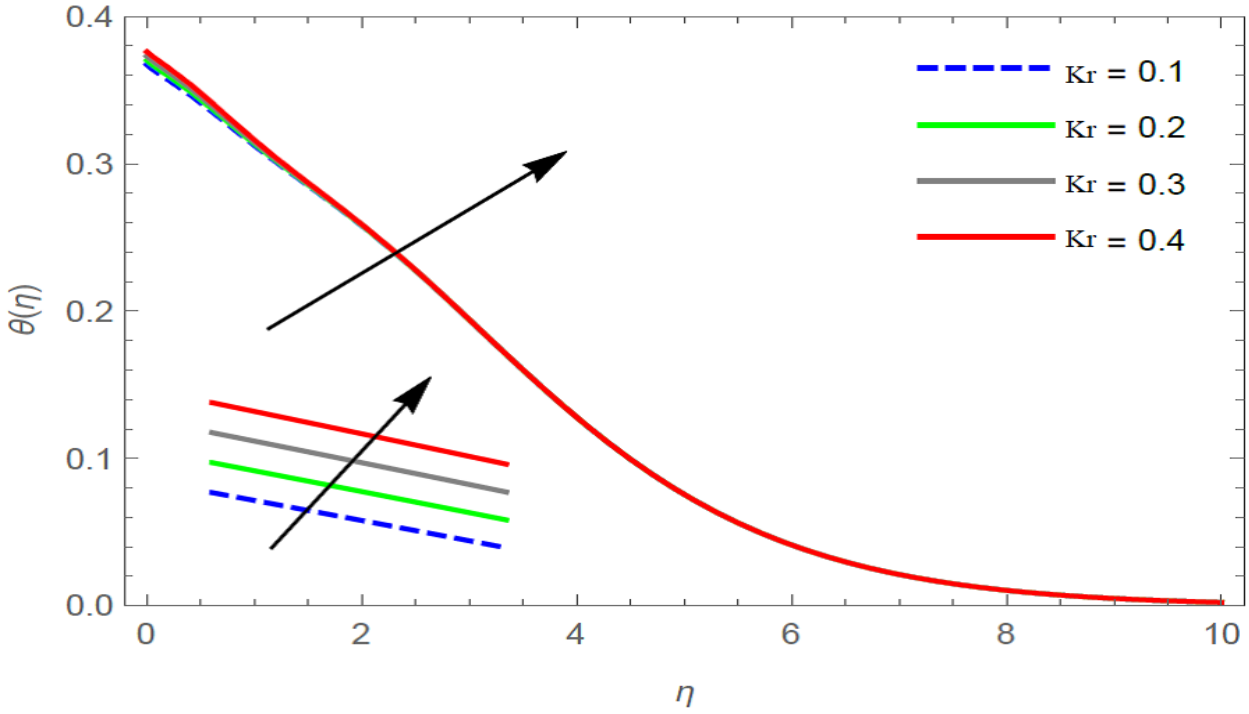

Figure 5.7: θ for η and Kr at $M = 1.2,\ s = 0.01,\ Nt = 0.2,\ Nb = 0.2,\ Le = 0.5,\ K = 0.05,$ $Pr = 6.7,\ Bi = 0.1,\ R = 2.0.$

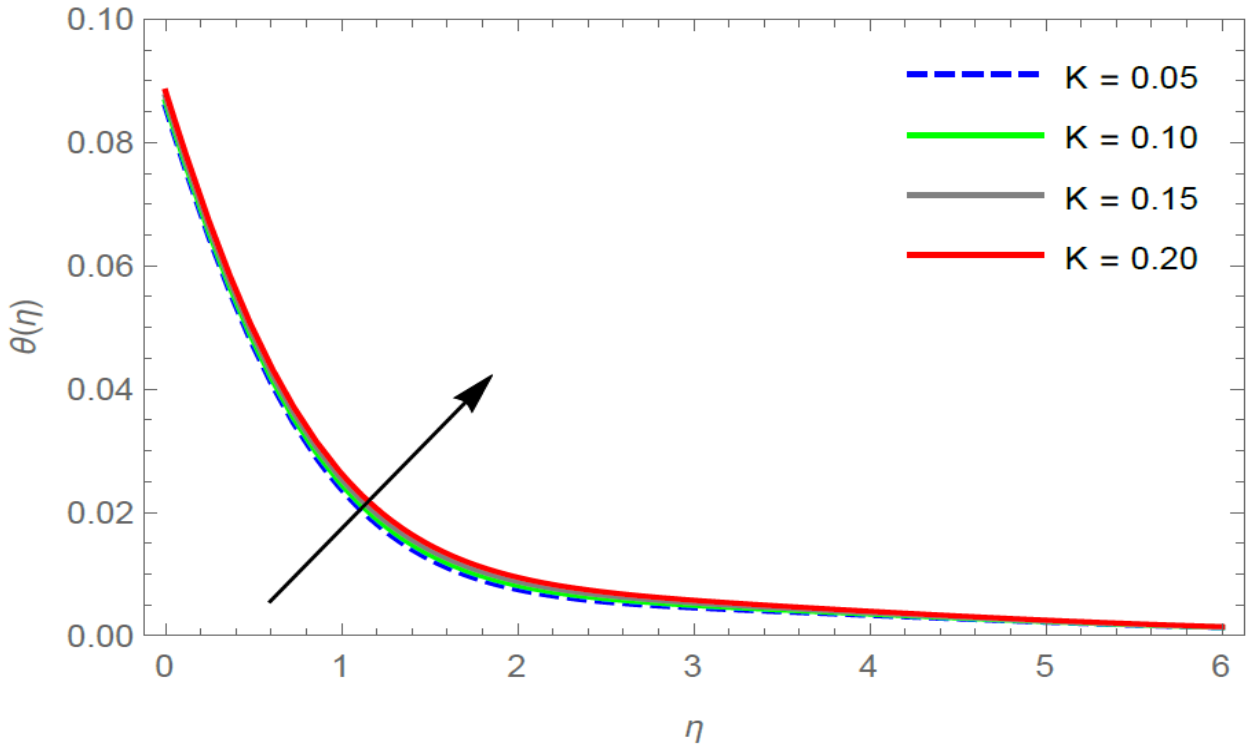

Figure 5.8: θ for η and K at $M = 1.2,\ Bi = 0.1,\ s = 0.01,\ Nt = 0.2,\ Nb = 0.2,\ Le = 0.5, Pr = 6.7,\ Kr = 0.2\ , R = 2.0.$

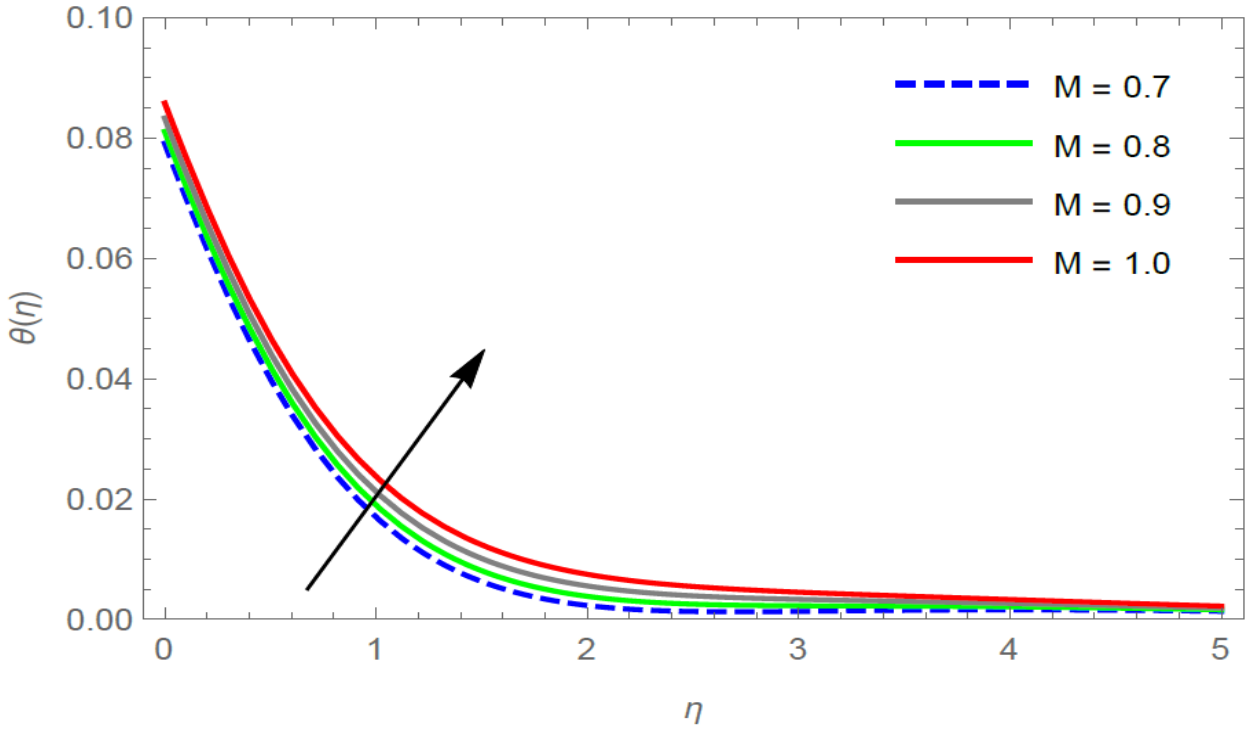

Figure 5.9: θ for η and M at $Le = 0.5,\ Bi = 0.1,\ s = 0.01,\ Nt = 0.2,\ Nb = 0.2,\ K = 0.05,$ $Pr = 6.7,\ Kr = 0.2,\ R = 2.0.$

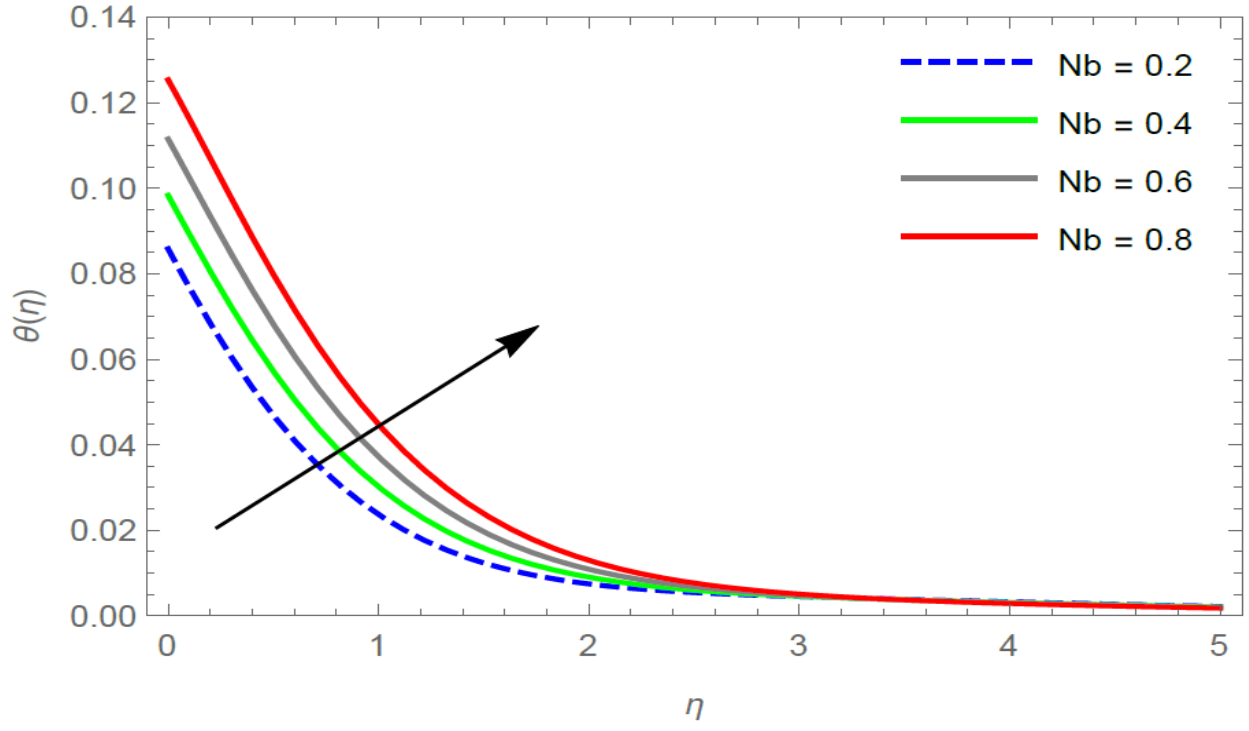

Figure 5.10: θ for η and Nb at $M = 1.2,\ Bi = 0.1,\ s = 0.01,\ Nt = 0.2,\ Le = 0.5,\ K = 0.05,$ $Pr = 6.7,\ Kr = 0.2, R = 2.0.$

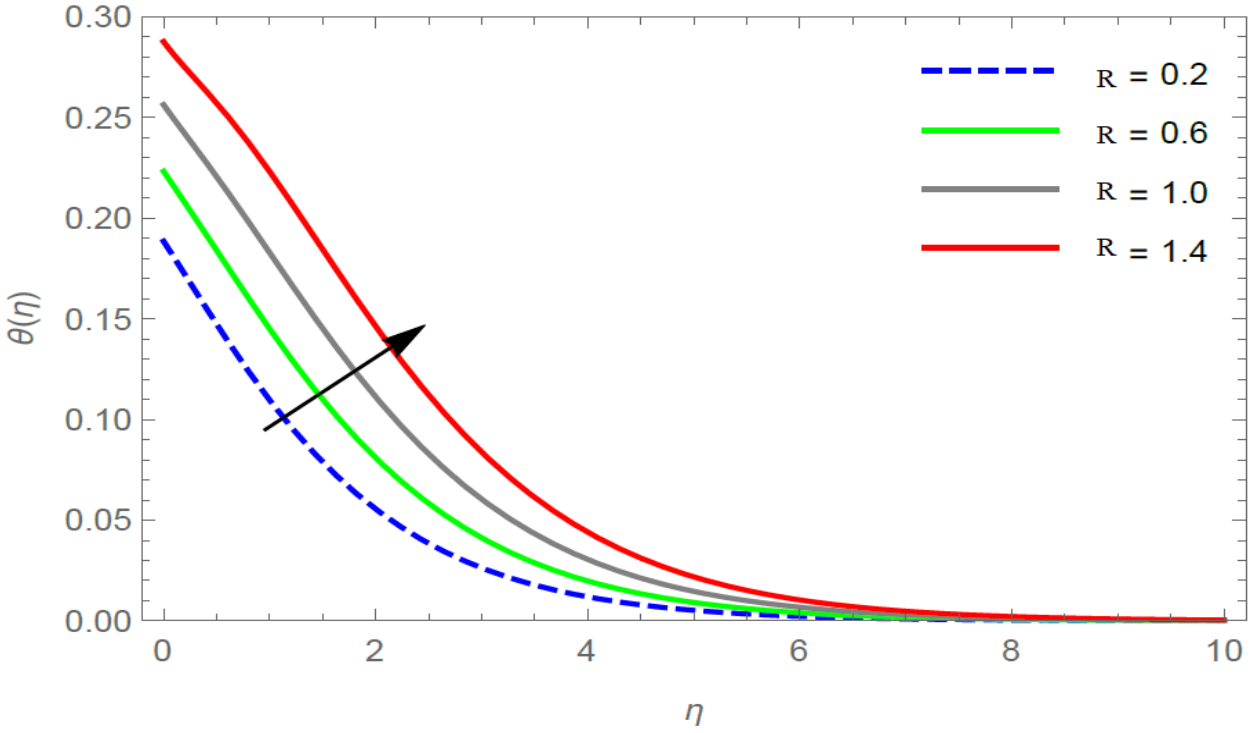

Figure 5.11: θ for η *and* R at $M = 1.2,\ Bi = 0.1,\ Nb = 0.2,\ Nt = 0.2,\ Le = 0.5,\ K = 0.05,$ $Pr = 6.7,\ s = 0.01\ ,\ Kr = 0.2.$

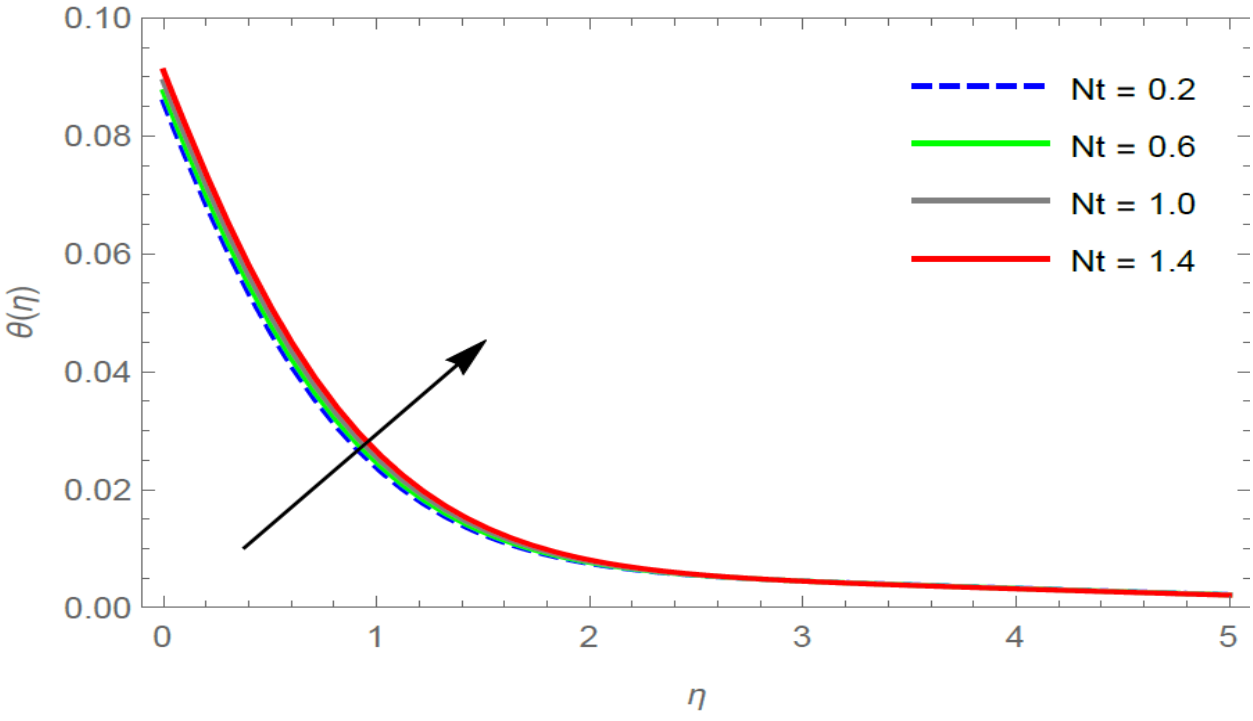

Figure 5.12: θ for η *and* Nt at $M = 1.2,\ Bi = 0.1,\ s = 0.01,\ Nb = 0.2,\ Le = 0.5,$ $K = 0.05,\ Pr = 6.7, Kr = 0.2\ , R = 2.0.$

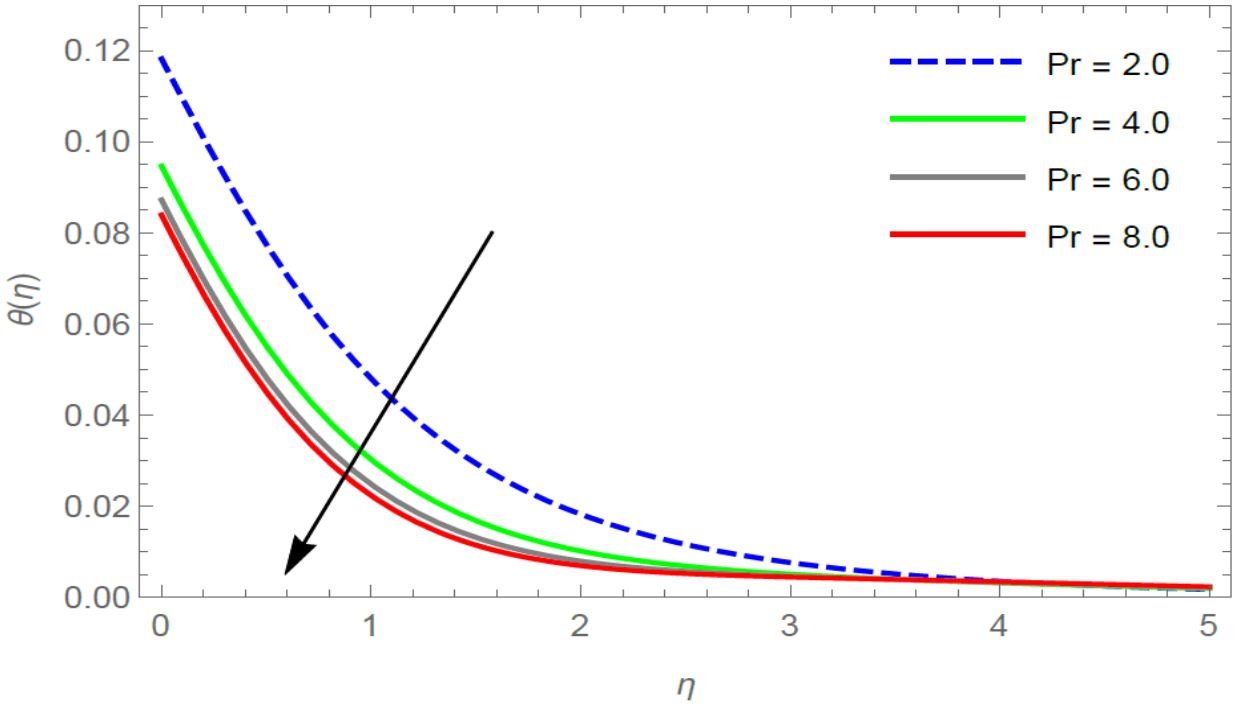

Figure 5.13: θ for η and Pr at $M = 1.2,\ Bi = 0.1,\ s = 0.01,\ Nt = 0.2,\ Le = 0.5,\ K = 0.05,$ $Nb = 0.2,\ Kr = 0.2\ , R = 2.0.$

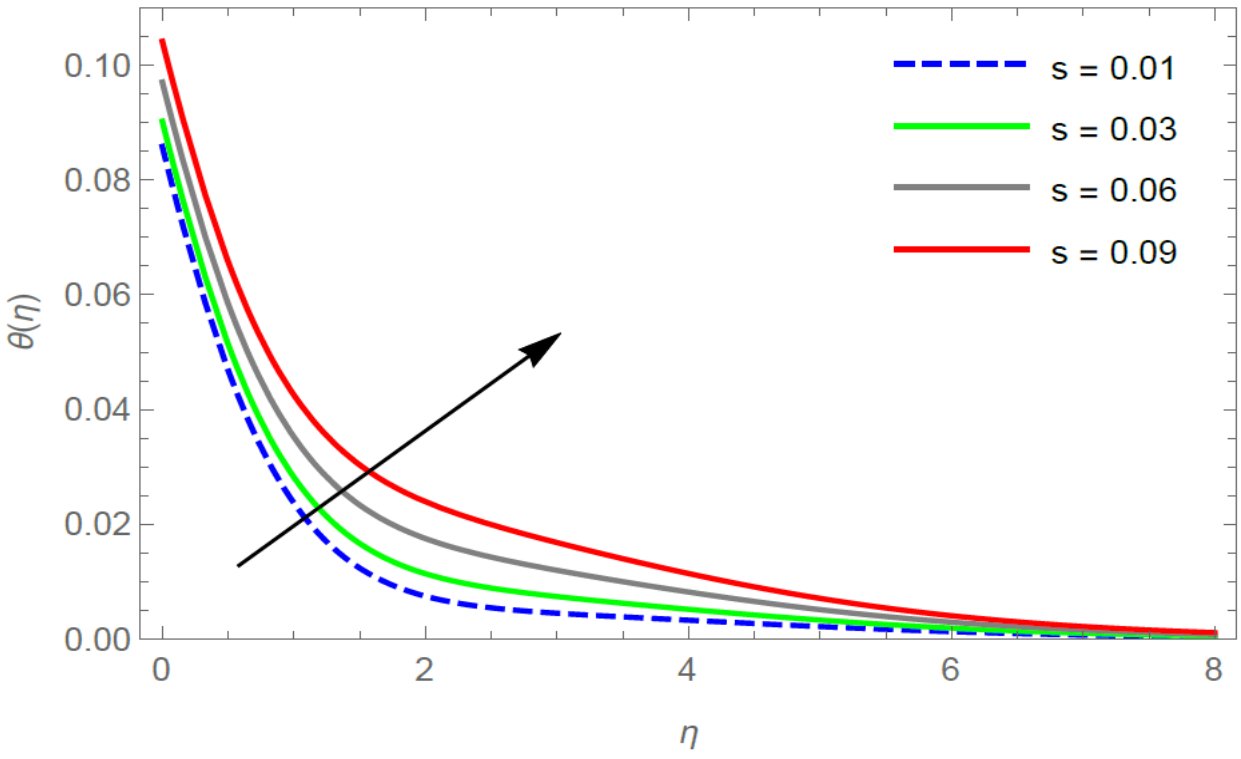

Figure 5.14: θ for η and s at $M = 1.2,\ Bi = 0.1,\ Nb = 0.2,\ Nt = 0.2,\ Le = 0.5,\ K = 0.05,$ $Pr = 6.7,\ Kr = 0.2\ ,\ R = 2.0.$

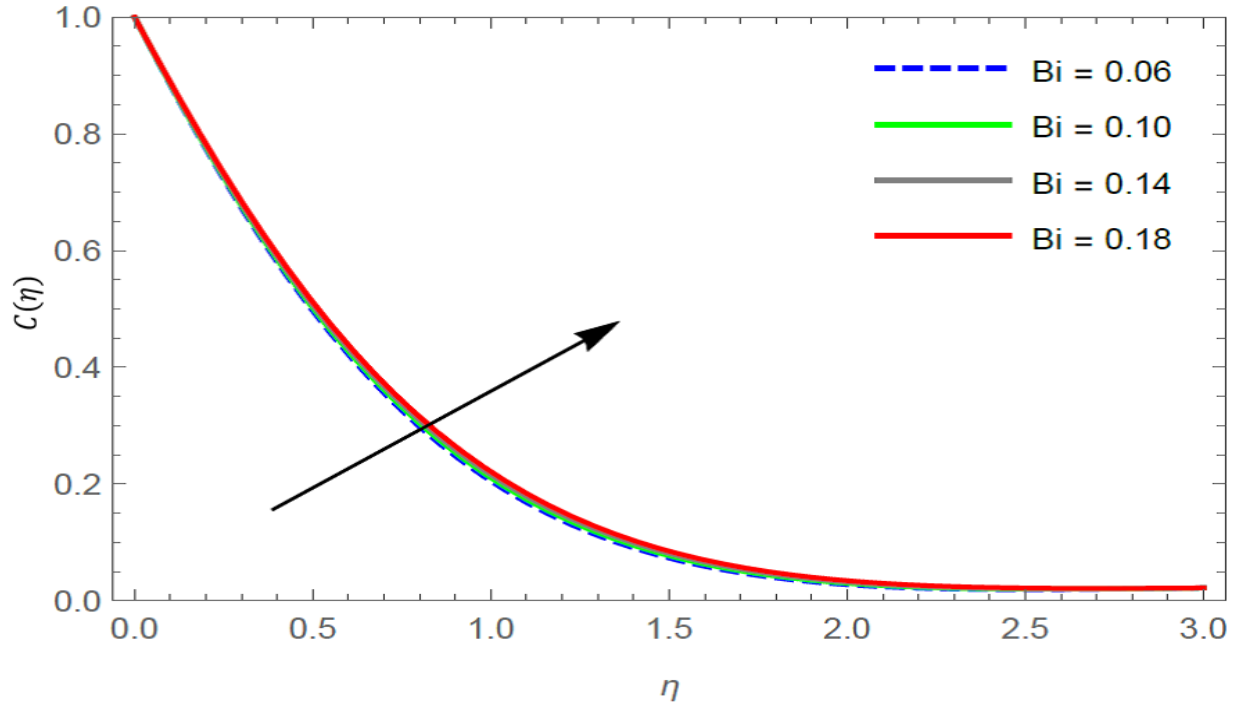

Figure 5.15: C for η and Bi at $M = 1.2,\ Nb = 0.2,\ Nt = 0.2,\ Le = 0.5,\ K = 0.05,\ Pr = 6.7,\ s = 0.01\ ,\ Kr = 0.2, R = 2.0.$

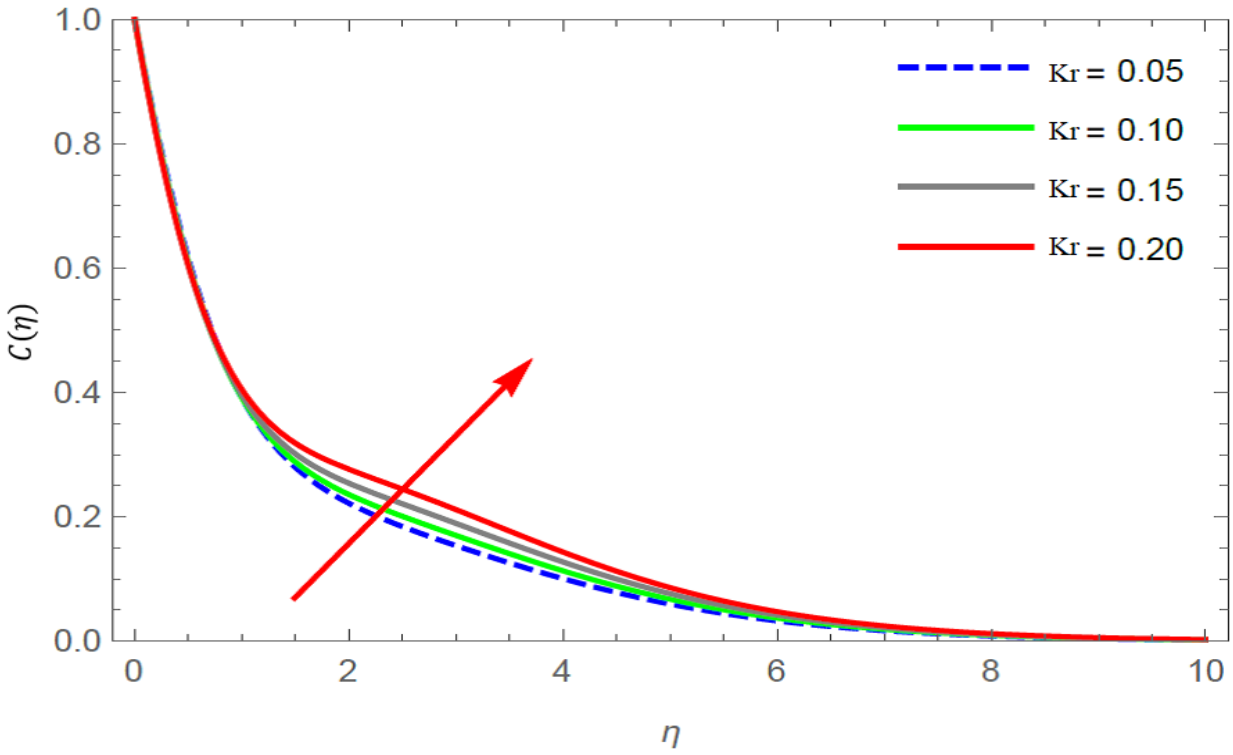

Figure 5.16: C for η and Kr at $Le = 0.5,\ Bi = 0.1,\ Nb = 0.2,\ Nt = 0.2,\ K = 0.05,\ Pr = 6.7,\ s = 0.01\ , M = 1.2,\ R = 2.0.$

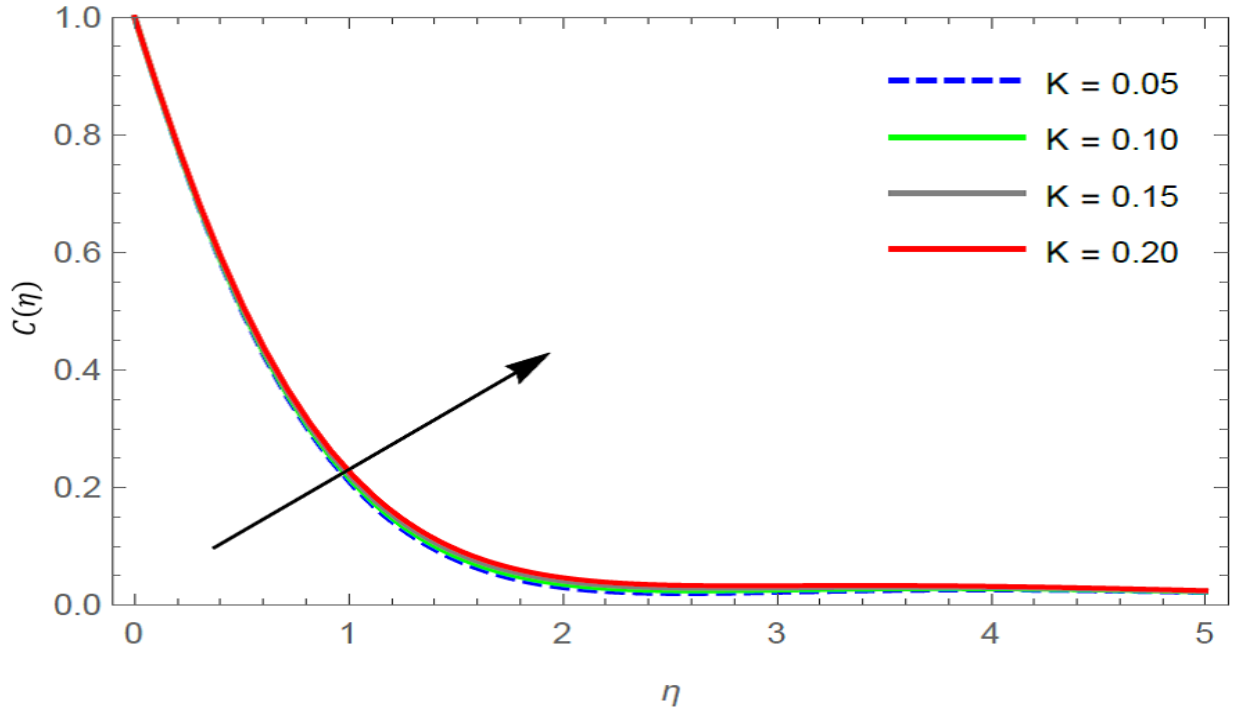

Figure 5.17: C for η and K at $M = 1.2,\ Bi = 0.1,\ Nb = 0.2,\ Nt = 0.2,\ Le = 0.5,\ Pr = 6.7,$ $s = 0.01\ ,\ Kr = 0.2,\ R = 2.0.$

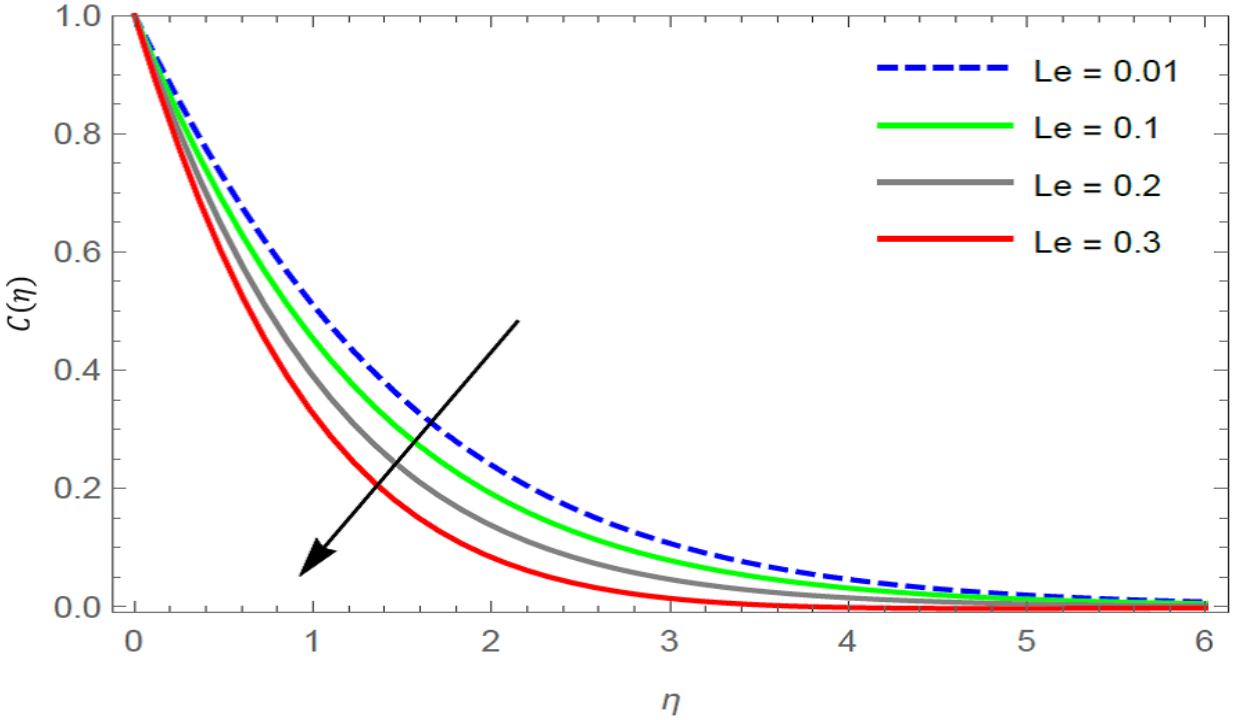

Figure 5.18: C for η and Le at $M = 1.2,\ Bi = 0.1,\ Nb = 0.2,\ Nt = 0.2,\ K = 0.05,\ Pr = 6.7,$ $s = 0.01\ ,\ Kr = 0.2,\ R = 2.0.$

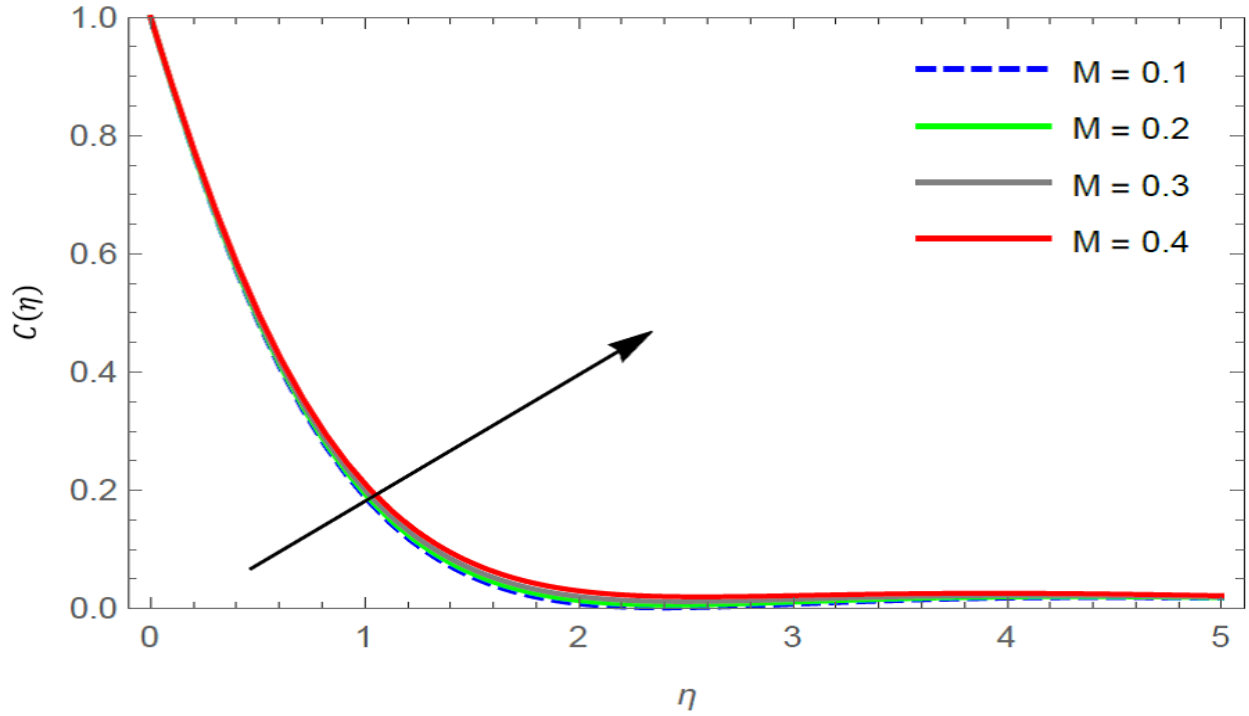

Figure 5.19: C for η and M at $Le = 0.5,\ Bi = 0.1,\ Nb = 0.2,\ Nt = 0.2,\ K = 0.05,\ Pr = 6.7,$ $s = 0.01\ , Kr = 0.2,\ R = 2.0.$

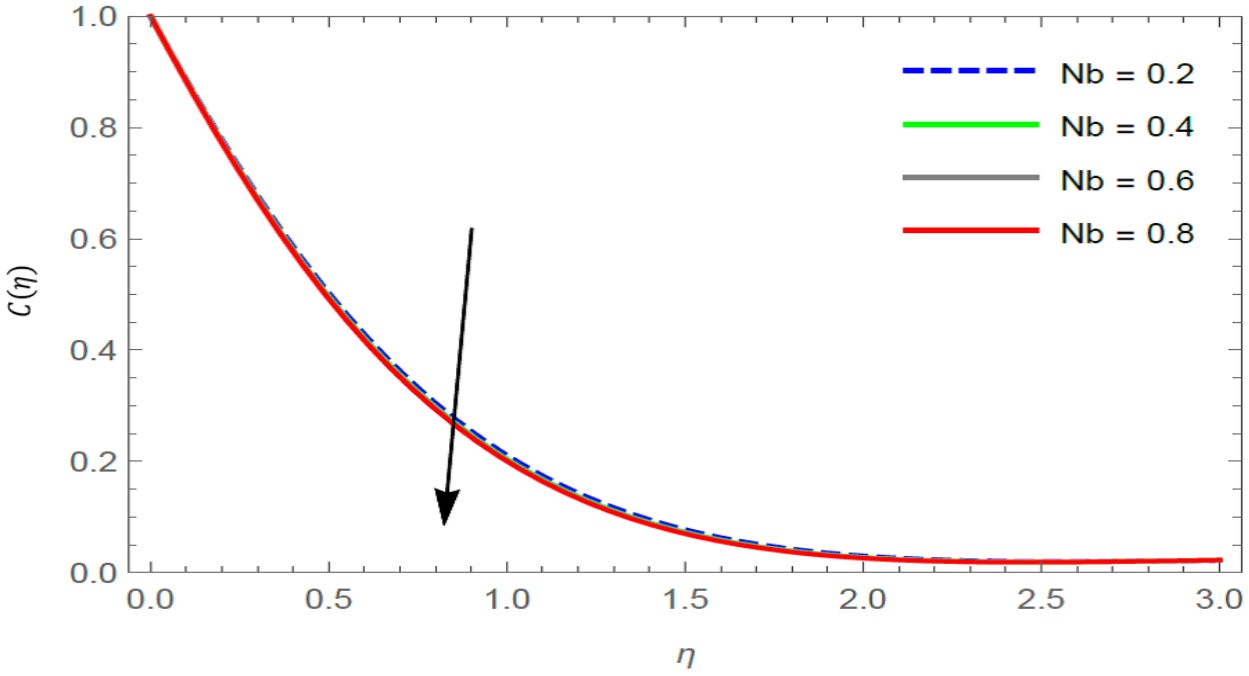

Figure 5.20: C for η and Nb at $Le = 0.5,\ Bi = 0.1,\ M = 1.2,\ Nt = 0.2,\ K = 0.05,\ Pr = 6.7,$ $s = 0.01\ ,\ Kr = 0.2,\ R = 2.0.$

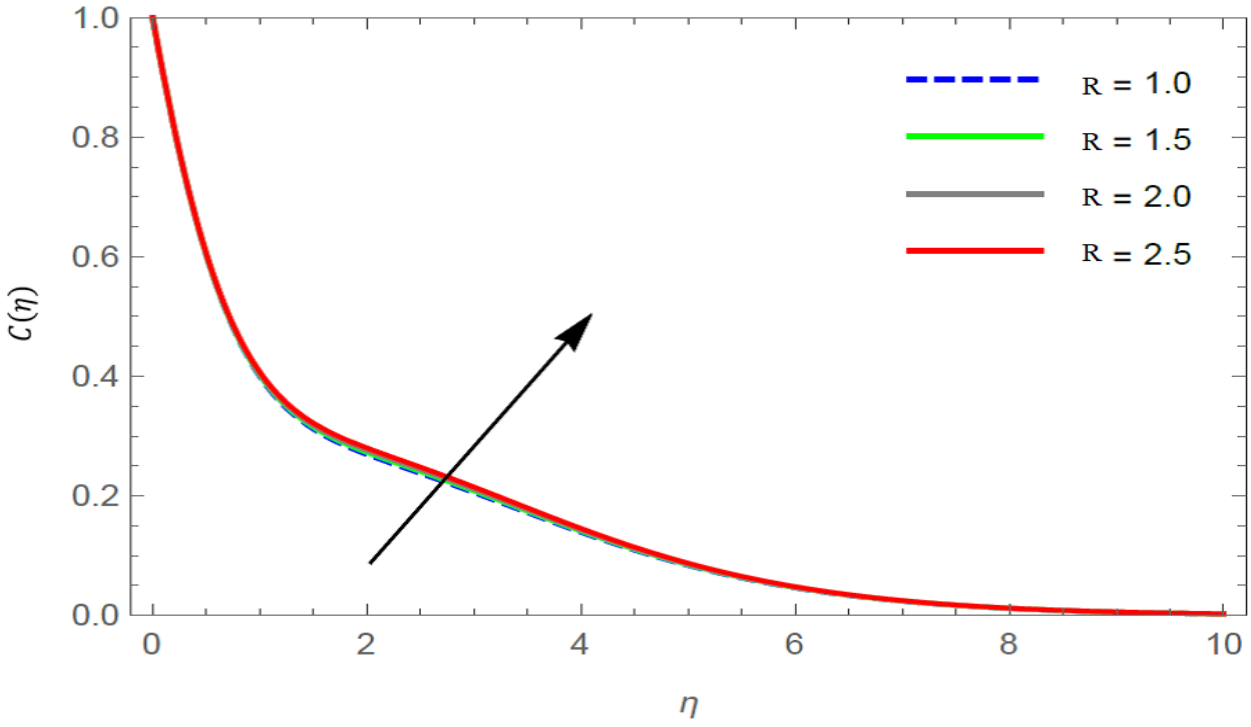

Figure 5.21: C for η *and* R at Le $= 0.5$, Bi $= 0.1$, Nb $= 0.2$, Nt $= 0.2$, K $= 0.05$, $Pr = 6.7$, $s = 0.01$, M $= 1.2$, $Kr = 0.2$

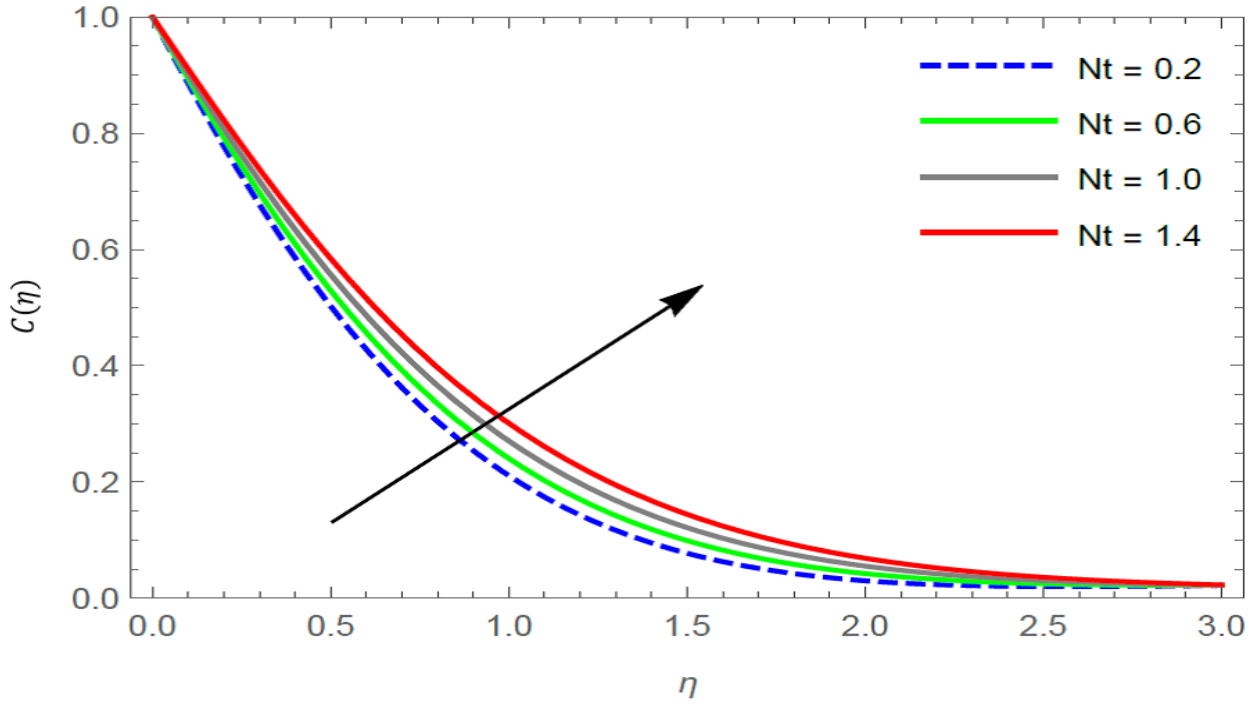

Figure 5.22: C for η *and* Nt at $Le = 0.5$, $Bi = 0.1$, $Nb = 0.2, M = 1.2$, $K = 0.05$, $Pr = 6.7$, $s = 0.01$, $Kr = 0.2$, $R = 2.0$.

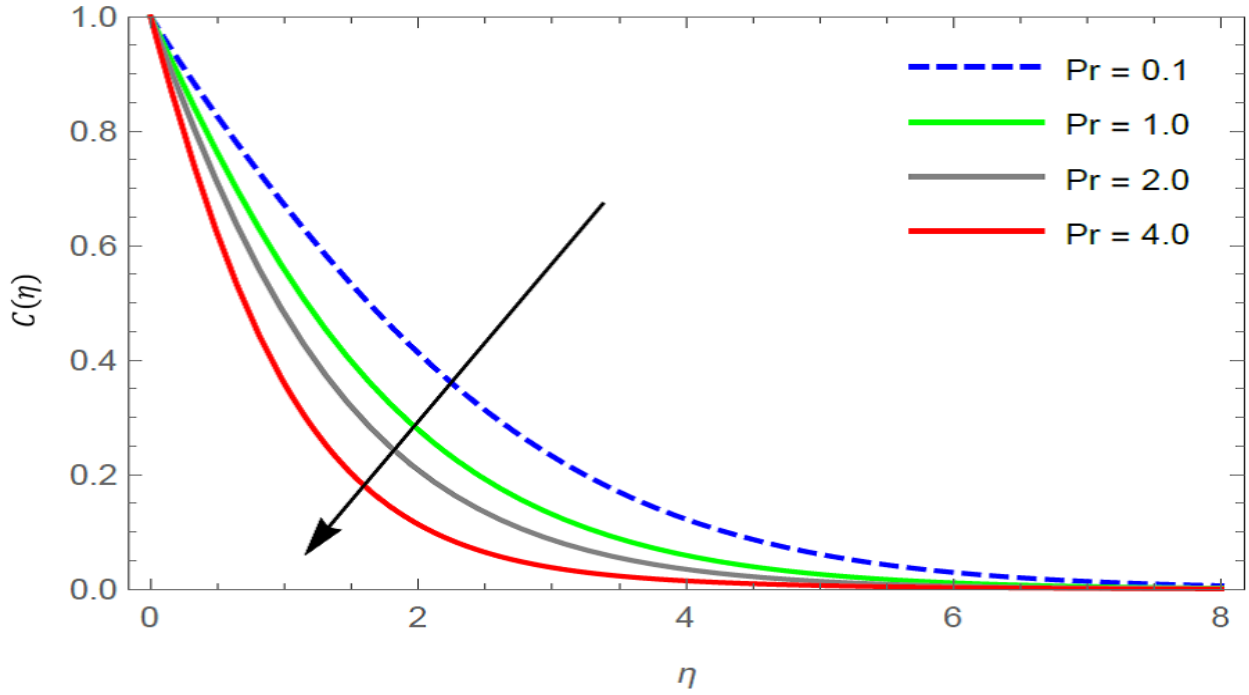

Figure 5.23: C for η and Pr at $Le = 0.5,\ Bi = 0.1,\ Nb = 0.2,\ Nt = 0.2,\ K = 0.05,\ M = 1.2,$ $s = 0.01\ ,\ Kr = 0.2,\ R = 2.0.$

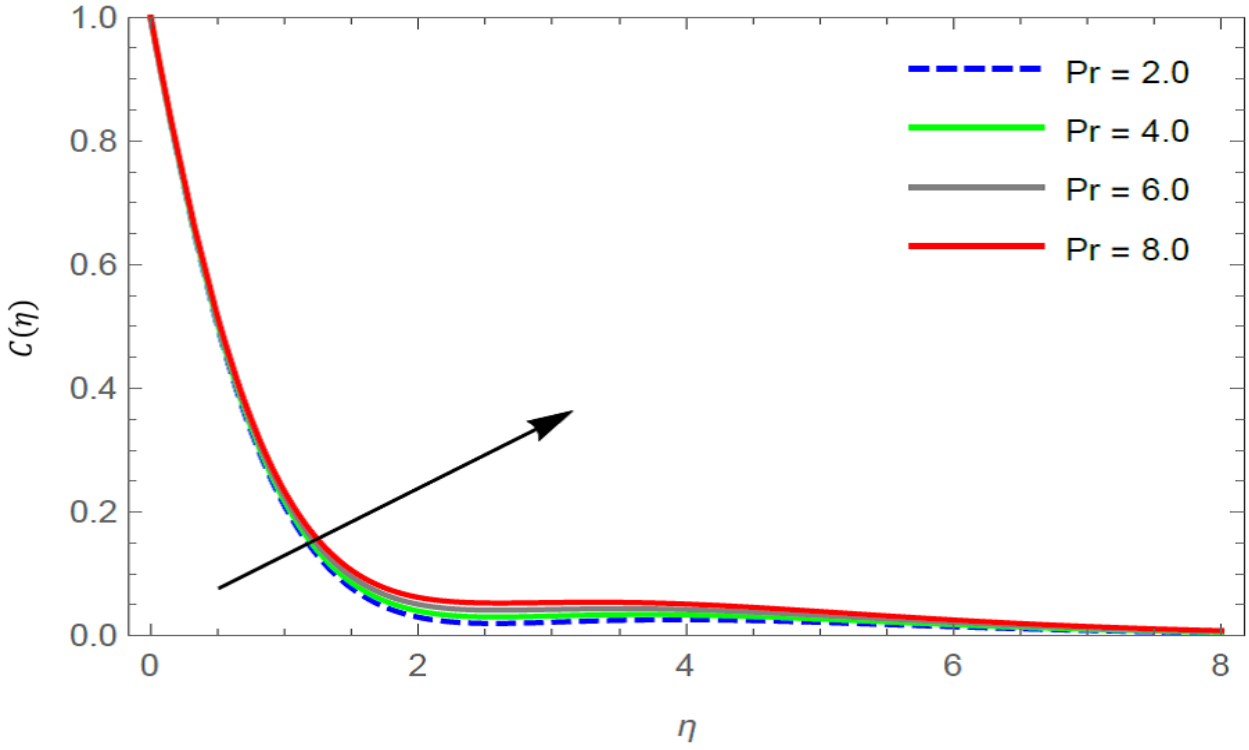

Figure 5.24: C for η and s at $Le = 0.5,\ Bi = 0.1,\ Nb = 0.2,\ Nt = 0.2,\ K = 0.05,\ Pr = 6.7,$ $M = 1.2\ ,\ Kr = 0.2,\ R = 2.0.$

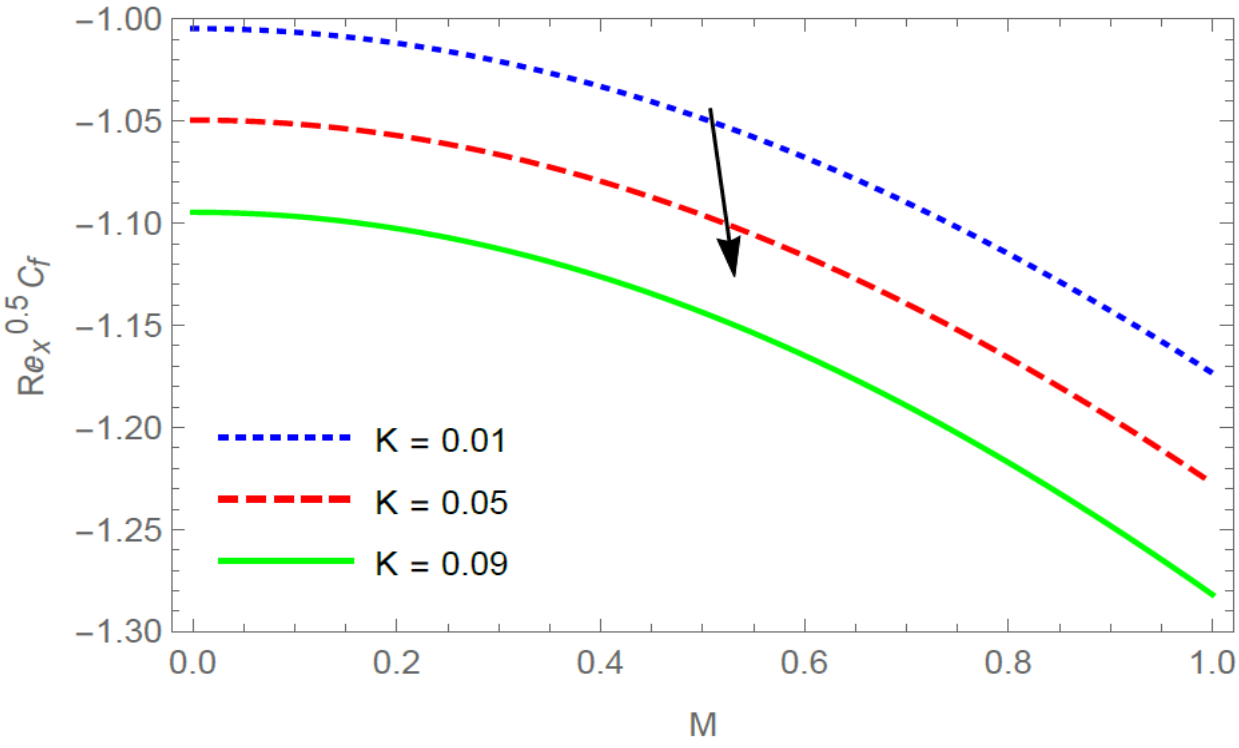

Figure 5.25: Effect of Viscoelastic parameter K on Skin friction coefficient at $Le = 0.5,\ Bi = 0.1,\ Nb = 0.2,\ Nt = 0.2,\ Pr = 6.7,\ s = 0.01\ , Kr = 0.2,\ R = 2.0.$

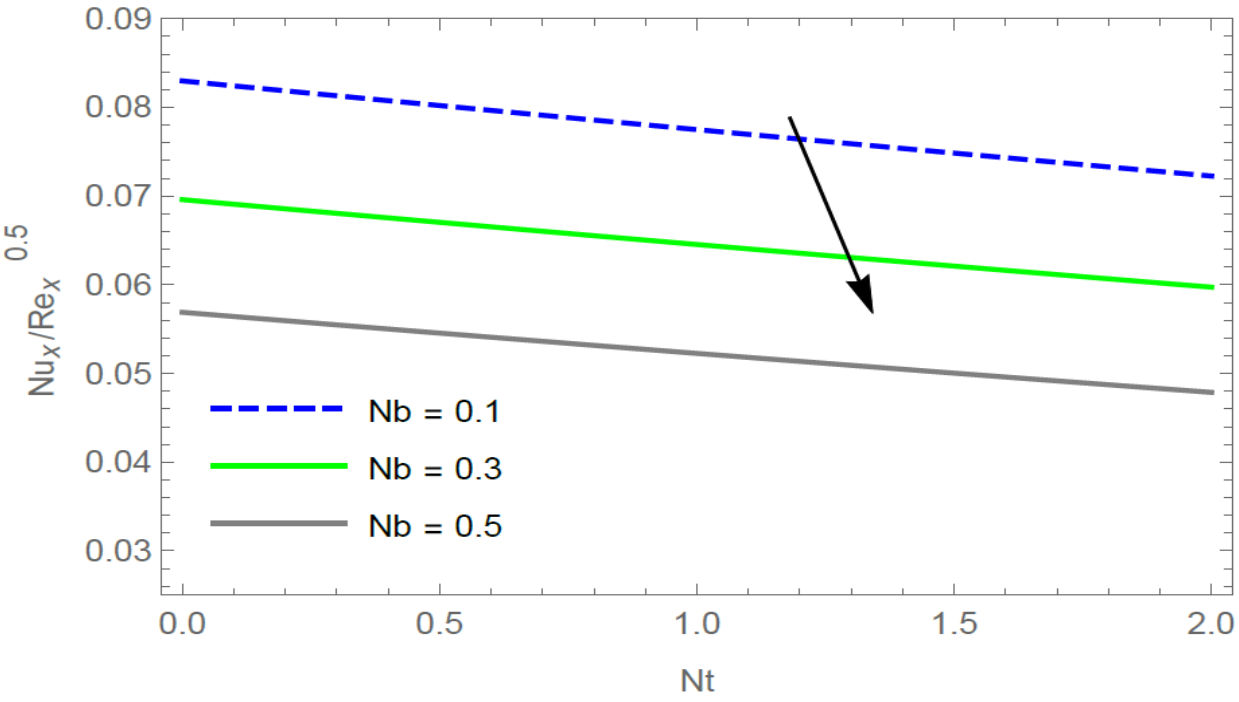

Figure 5.26: Effect of Brownian motion parameter Nb on the Nusselt number at $Le = 0.5,\ Bi = 0.1,\ M = 1.2,\ K = 0.05,\ Pr = 6.7,\ s = 0.01\ , Kr = 0.2, R = 2.0.$

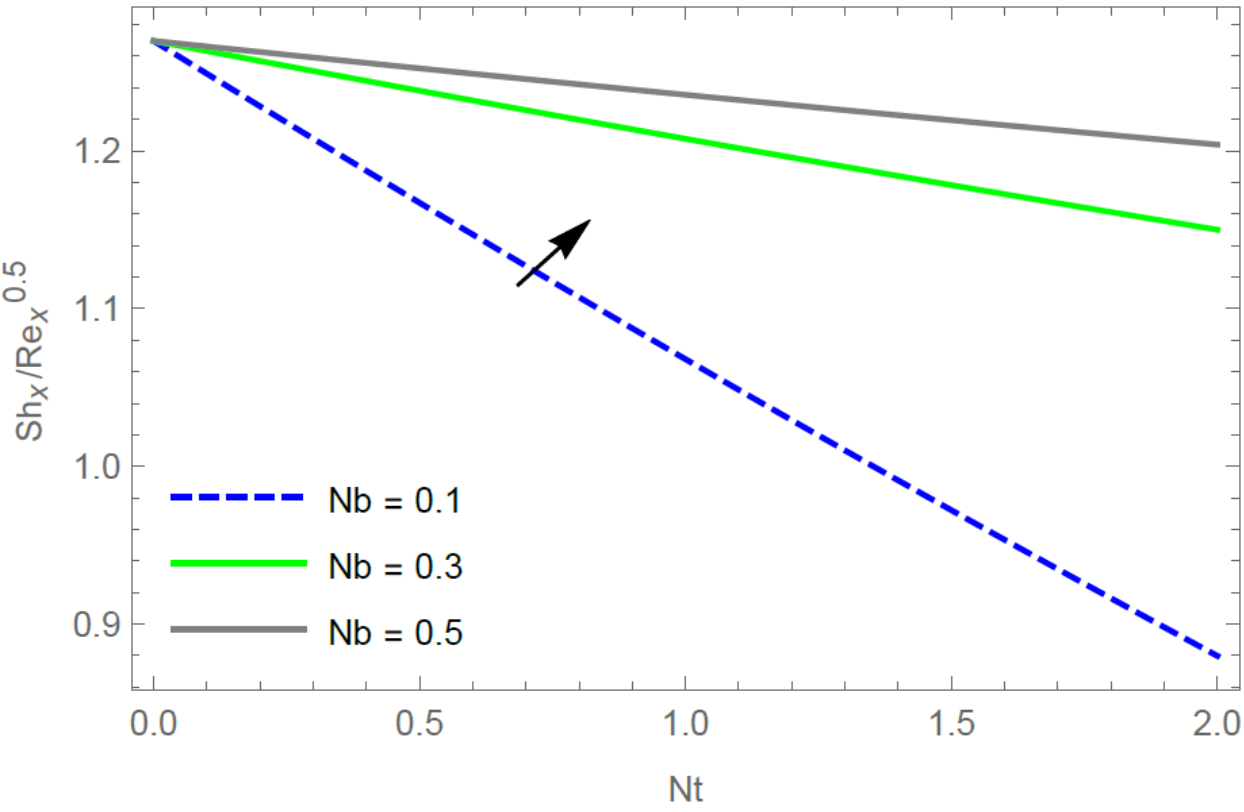

Figure 5.27: Effect of Brownian motion parameter Nb on Sherwood number at $Le = 0.5,\ Bi = 0.1,\ M = 1.2,\ K = 0.05,\ Pr = 6.7,\ s = 0.01\ , Kr = 0.2, R = 2.0$

Effect of Radiation Parameter R on concentration profile is depicted in figure 5.21. It can be observed that concentration increases as radiation parameter increases. Figure 5.22 represents a concentration field via Thermophoresis parameter Nt. It is observed that as thermophoresis parameter Nt rises, concentration increases. By Figure 5.23, the effect of Prandtl number on concentration profile can be observed. Here concentration reduces as Prandtl number Pr increases. It is noticeable in Figure 5.24 that as stagnation parameter increases, the concentration increases. Figure 5.25 shows the changes in skin friction coefficient with Viscoelastic fluid parameter K. It is observed that skin friction reduces with increase in viscoelastic parameter. Figure 5.26-5.27 depict the effect of Brownian parameter on Nusselt number and the Sherwood number respectively.

It is noticeable from Figure 5.26 that as Brownian motion parameter Nb rises, Nusselt number reduces. It is also observed from Figure 5.27 that increasing values of Nb has positive impact on the Sherwood number.

5.6 Conclusion:

The objective of this research is to obtain semi–analytic solution for two dimensional Viscoelastic fluid flow and observe thermophoresis, Brownian motion, radiation and chemical reaction effects. Key remarks for the conclusions can be summarized as follows.

- Fluid velocity declines with K and M.
- Fluid velocity surges with s.
- Fluid temperature can be amplified by increasing either Bi, Kr, K, M, Nb, Nt, R or s.
- Fluid temperature decreases with increasing values of Pr
- Skin friction reduces on increasing K.
- Nb has positive impact on the Sherwood number.
- Nusselt number decreases with increase in Nb.